Scanning tunneling microscopy of epitaxial $YBa_2Cu_3O_{7-x}$ films prepared by thermal plasma flash evaporation method

Kei Hayasaki, Yuzuru Takamura,[a] Norio Yamaguchi,[b] Kazuo Terashima, and Toyonobu Yoshida
Department of Metallurgy and Materials Science, Graduate School of Engineering, The University of Tokyo, Hongo 7-3-1, Bunkyo-ku, Tokyo 113, Japan

(Received 12 August 1996; accepted for publication 24 October 1996)

The surface morphology of epitaxial $YBa_2Cu_3O_{7-x}$ films prepared by thermal plasma flash evaporation was extensively investigated by scanning tunneling microscopy. Under epitaxial film growth conditions with the deposition rate up to 0.42 μm/min, two-dimensional nucleus growth and spiral growth were observed. The main deposition species in this process was found to be the cluster ranging from 0.3 to 9 nm and the size of the cluster influenced the growth mode strongly. Theoretical analysis based on the two-dimensional critical radius revealed that smaller clusters became weakly bonded nuclei resulting in spiral growth and larger clusters became stable nuclei resulting in two-dimensional nucleus growth, which we named two-dimensional cluster nucleus growth. The clusters generated in the plasma boundary layer undoubtedly involve sufficient energy necessary for crystallization and show quite different characteristics from those of the clusters generated in vacuum by adiabatic expansion process. Hence, this process must be named ''hot cluster epitaxy.'' © *1997 American Institute of Physics.* [S0021-8979(97)04203-5]

I. INTRODUCTION

The discovery of high T_c (superconducting transition temperature) superconductors such as $YBa_2Cu_3O_{7-x}$ (T_c = 92 K),[1] $Bi_2Sr_2Ca_2Cu_3O_{10}$ (105 K),[2] $Tl_2Ba_2Ca_2Cu_3O_{10}$ (120 K)[3] has resulted in the development of many novel processes for the preparation of their high-quality thin films. In particular, $YBa_2Cu_3O_{7-x}$ (YBCO) films with a high critical current density (J_c) of more than 10^6 A/cm^2 at 77 K have been successfully obtained by various methods such as sputtering,[4] laser ablation,[5] thermal coevaporation,[6] and chemical vapor deposition (CVD).[7]

The plasma flash evaporation method developed by our group[8–11] is a promising method for the preparation of epitaxial YBCO films. It has some interesting characteristics such as high rate (300 nm/s) and large area (7×7 cm^2) deposition under high flux of atomic oxygen (10^{19} atoms/cm^2 s).[12] This process is inferred to be characterized by cluster deposition under high flux of atomic oxygen.[13] Nanometer-scale clusters are formed in the boundary layer under the high supersaturation caused by quenching from 5000 to 1000 K (Fig. 1). The cluster size can be controlled between 0.3 and 9 nm by controlling the quenching rate and concentration of vapor phase species.[12] Clusters have a larger sticking probability than atoms and can easily be attached to a crystal surface. [12] This may be one of the reasons for such a high deposition rate. Very recently, a scanning tunneling microscopy (STM) study relating to the growth feature of YBCO films in this process has been reported by Tsujino *et al.*[14] However, the cluster deposition has not been explained clearly.

In this article, the YBCO films deposited on $SrTiO_3$(100) by thermal plasma flash evaporation method were extensively investigated by STM. Lateral growth mechanism of the epitaxial films from clusters will be discussed.

II. EXPERIMENT

The plasma flash evaporation apparatus for depositing YBCO films has been described elsewhere.[12] The substrate temperature was measured using a thermocouple 1 mm below the substrate. The experimental conditions are listed in Table I.

All the films used in this study showed c-axis orientation, in-plane orientation, and a sharp superconducting transition at a temperature T_c above 87 K with a narrow transition width of 1 K. The surface morphology of YBCO films was investigated by STM (Nanoscope II, Digital Instruments). All STM measurements were carried out in the constant-current mode at room temperature in air. Etched Pt–Ir scanning tips were employed. The tunneling current and the bias voltage were 0.2 nA and 800 mV, respectively.

III. RESULTS

The cluster size measured by the microtrench method was estimated to be 0.3–9 nm[12] on the average. In order to measure the cluster size directly, we observed clusters deposited on highly oriented pyrolytic graphite (HOPG) substrates by STM. Fig. 2 shows a schematic diagram of the cluster trapping apparatus, which is the same as that used for the measurement of atomic oxygen flux.[12] Fig. 3(a) shows a lattice image of a HOPG substrate exposed to oxygen plasma without powder feeding for a very short time (0.02 s) which indicates that the HOPG substrate was not damaged by the oxygen plasma in such a short period. Fig. 3(b) shows an STM image of YBCO clusters trapped in the same period, the diameter and height of which are 6 and 0.7 nm, respectively. This image reconfirms that the deposition species in this process is the cluster.

[a]Present address: The Institute of Space and Astronautical Science, 3-1-1, Yoshinodai, Sagamihara-shi, Kanagawa 229, Japan. Electronic mail: takamura@peter.materials.isas.ac.jp
[b]Electronic mail: norio@plasma.t.u-tokyo.ac.jp

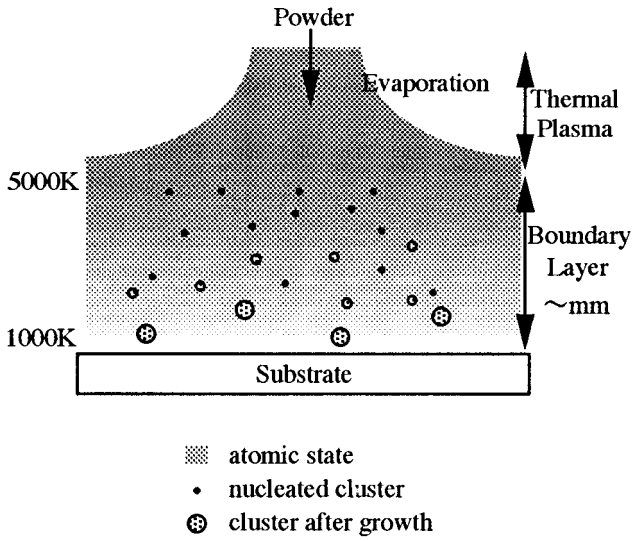

FIG. 1. The concept of cluster deposition in the plasma flash evaporation process.

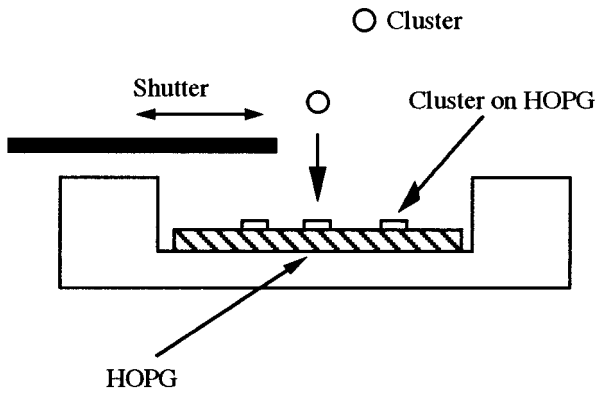

FIG. 2. A schematic diagram of the cluster trapping apparatus.

We performed the STM measurement of YBCO films deposited on $SrTiO_3(100)$ substrates at various substrate temperatures (T_{sub}), feeding rates (R), and distance between the torch exit and the substrate (L) as listed in Table I. The films with R = 60 mg/min (T_{sub} = 700 to 660 °C) and $R=150$ mg/min (T_{sub} = 695 to 670 °C) show spiral growth originated from the edges of the screw dislocations at the substrate surfaces and the vertical step height is equal to one unit cell (1.2 nm). This morphology is frequently reported in other methods such as sputtering[15,16] and CVD.[17] Therefore, the spiral growth mechanism is considered to be a general one regardless of the film deposition method. In the case of $R=60$ mg/min, the terrace widths λ decrease from 130 to 65 nm with decreasing T_{sub} from 700 to 660 °C. In the case of $R=150$ mg/min, the terrace widths decrease from 110 to 55 nm with decreasing T_{sub} from 695 to 670 °C. STM images of the surfaces are shown in Figs. 4(a)–4(e). The cases (a)–(d) clearly show spiral growth. On the other hand, in the case of $R=200$ mg/min (Fig. 4(e)), the spiral growth feature is not observed and is irregular in shape, but still regular 1.2 nm step-height terraces are observed. These facts indicate that this film grew with a non-spiral epitaxial growth like normal two-dimensional nucleus growth (2DNG). As described later, we call this growth mode 2D cluster nucleus growth (2DCNG) in order to stress the difference between 2DNG and this 2DNG mechanism.

TABLE I. Experimental conditions.

rf power	50 kW
Pressure	200 Torr
Plasma O_2 gas	47 standard liter per minute (SLM)
Carrier Ar gas	2.4 SLM
Feeding rate (R)	60–200 mg/min
Torch-substrate distance (L)	260–310 mm
Substrate temperature (T_{sub})	660–700 °C
Deposition time	0.5–2 min

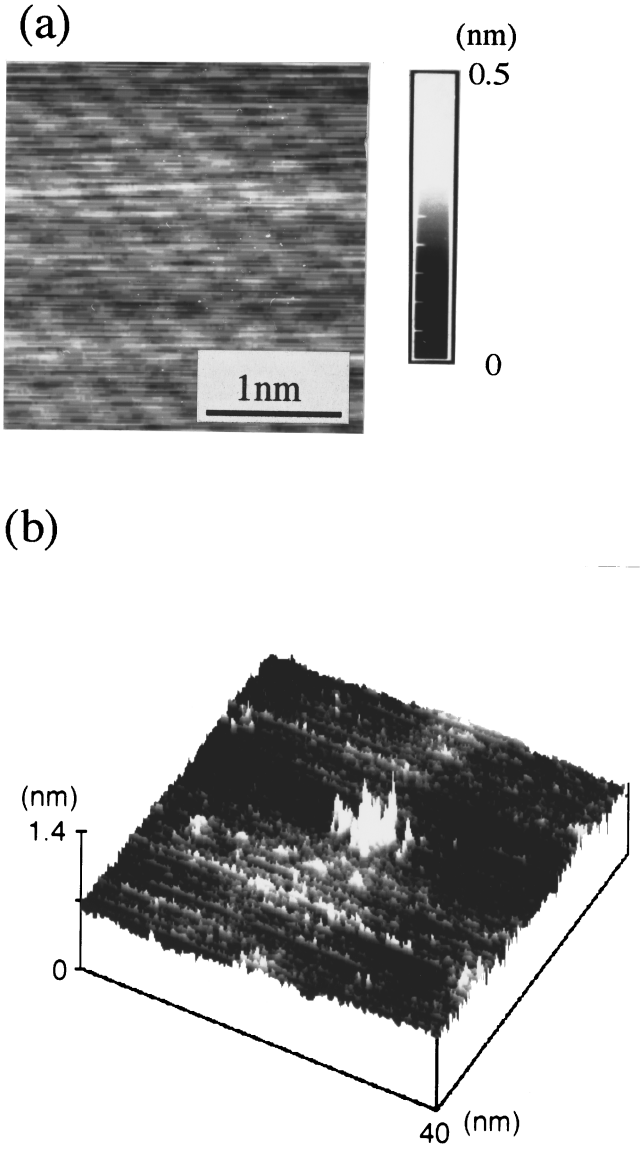

FIG. 3. (a) A lattice image of a HOPG substrate exposed to oxygen plasma without powder feeding. (b) An STM image of clusters on a HOPG substrate.

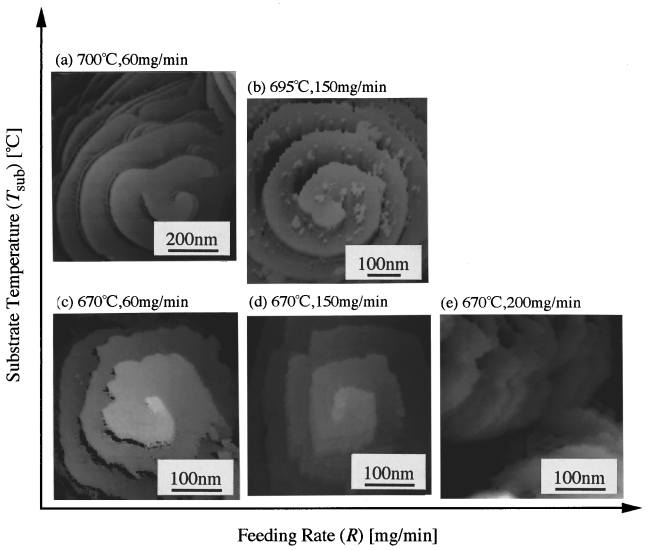

FIG. 4. STM images of YBCO films grown on $SrTiO_3$(100) (L = 310 mm). (a) R=60 mg/min, T_{sub} = 700 °C, (b) R=150 mg/min, T_{sub} = 695 °C, (c) R=60 mg/min, T_{sub} = 670 °C, (d) R=150 mg/min, T_{sub} = 670 °C, and (e) R=200 mg/min, T_{sub} = 670 °C.

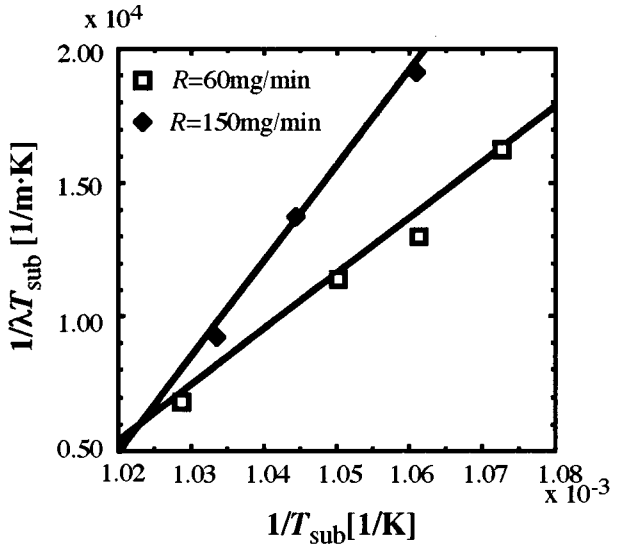

FIG. 5. Plots of $1/\lambda T_{sub}$ vs $1/T_{sub}$. λ and T_{sub} represent terrace width and substrate temperature.

IV. DISCUSSION

A. Terrace width dependence on substrate temperature

According to the BCF theory,[18] the terrace width (λ) in spiral growth is given by

$$\lambda \approx 20\rho_c = \frac{20\gamma a}{k_B T \ln \frac{p}{p_0}}, \tag{1}$$

where ρ_c, γ, a, k_B, T_{sub}, p and p_0 are the critical nucleus radius, the surface energy per unit cell, the lattice constant, Boltzmann constant, the substrate temperature, the actual vapor pressure and the equilibrium vapor pressure, respectively.

For the case of multicomponent systems, the definition p/p_0 is somewhat ambiguous. However, approximation $\ln p/p_0 \sim \ln J/J_0$ may not be so bad in this case, where J and J_0 are the feeding rate and the critical feeding rate at which film growth occurs, respectively. Using Eq. (1) and the value of λ measured by STM, we can estimate γ. From λ = 80 nm (R=60 mg/min) and λ = 55 nm (R=150 mg/min) at T_{sub}=700 °C, the value of γ is derived to be 1.6 J/m^2. This value is equal to that estimated by mechanical measurements.[19,20]

In addition, Eqs. (2)–(4) can be applied to the adsorbed particles, such as atoms, molecules and clusters:

$$J_o = \frac{n_{s0}}{\tau_s}, \tag{2}$$

$$n_{s0} = n_0 \exp\left(-\frac{W_s}{k_B T_{sub}}\right), \tag{3}$$

$$\frac{1}{\tau_s} = \nu \exp\left(-\frac{W_s'}{k_B T_{sub}}\right), \tag{4}$$

where n_{s0}, n_0, τ_s, ν, W_s and W_s' are concentration on a surface, concentration at a step, mean lifetime of an adsorbed particle, frequency of vibration, the evaporation energy from the kinks to the surface, and the evaporation energy from the surface to the vapor phase, respectively.

From Eqs. (1)–(4), we obtain

$$\frac{1}{\lambda T_{sub}} = \frac{k_B}{20\gamma a} \ln \frac{J}{\nu n_0} + \frac{W_s + W_s'}{20\gamma a} \frac{1}{T_{sub}}. \tag{5}$$

From the STM measurements, linear dependences of $1/\lambda T_{sub}$ on $1/T_{sub}$ would be derived as shown in Fig. 5. This means that the terrace width dependence on the substrate temperature can be explained using Eq. (5) on the assumption that the variation of $\ln J_o$ is negligible compared with the variation of $1/T_{sub}$. The sum of the evaporation energy from the kinks to the crystal surface and the re-evaporation energy from the crystal surface, $W_s + W_s'$, corresponds to the slope of the linear plots of $1/\lambda T_{sub}$ versus $1/T_{sub}$. The values at R=60 and 150 mg/min are estimated to be 1.8×10^{-19} and 3.1×10^{-19} J, respectively, for a=0.38 nm and γ=1.6 J/m^2.[19,20] $W_s + W_s'$ for R = 200 mg/min is 1.7 times larger than that for R = 60 mg/min. The difference of these values may be caused by that of absorbed species, probably caused by the difference in the cluster sizes. Increasing the sizes, the clusters can be absorbed to the substrate surface more strongly. Therefore, the value of $W_s + W_s'$ becomes greater. This result supports the idea that deposition from clusters is more effective in depositions than that from atoms and small clusters, especially at high substrate temperatures.

B. Lateral growth mechanism from clusters

Here, we discuss a mechanism by the comparison of the two-dimensional critical radius (r_{2D}^*) derived from the terrace width and the two-dimensional cluster size (r_{2D}) estimated from the three-dimensional cluster size (r_{3D}).

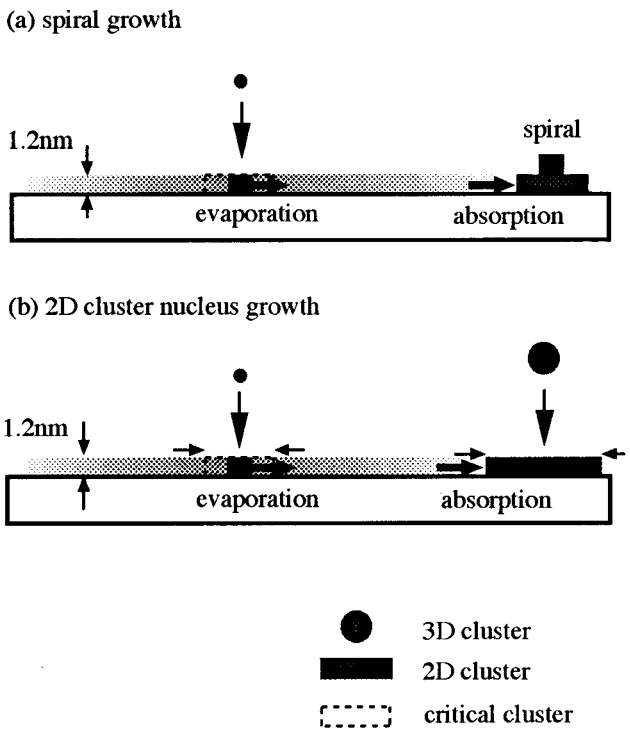

FIG. 6. Schematic description of the behavior of a cluster.

First, we assume that a cylindrical 2D cluster with a step height of 1.2 nm is rearranged on the crystal surface from a 3D cluster as shown in Fig. 6. According to the cluster size measurement,[12] the 3D cluster sizes (r_{3D}) generated in plasma at $L=310$ mm are 1, 1.6, 2 and 3 nm at the feeding rates $R=60$, 150, 200 and 350 mg/min, respectively. In these cases, the rearranged 2D cluster radiuses (r_{2D}) at each feeding rate are estimated to be 0.4, 0.8, 1.1 and 1.9 nm, respectively. The values of r_{2D} are plotted in Fig. 7. On the other hand, the 2D critical radius (r^*_{2D}) derived from Eq. (1) are 4 and 2.75 nm at $R=60$ and 150 mg/min, respectively. Under the assumption of a linear dependence of p to R and using

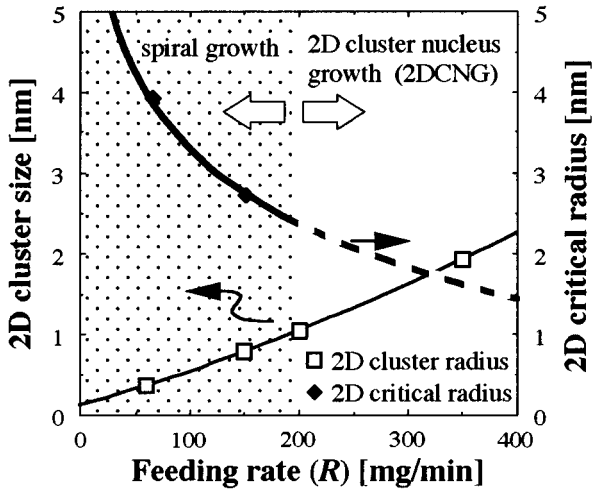

FIG. 7. The comparison of 2D cluster radius and 2D critical radius.

the two values of r^*_{2D}, the dependence of r^*_{2D} on R can be drawn as shown in Fig. 7. The clusters having r_{2D} larger than r^*_{2D} are considered to be stable on the surface. On the other hand, the clusters with $r_{2D} \ll r^*_{2D}$ should be evaporated onto the surface.

In the case of all the incoming clusters with the size $r_{2D} < r^*_{2D}$, the growth mode is expected to be almost the same as the case of the growth from the atoms causing the spiral growth. While increasing the feeding rate or decreasing the substrate temperature, the r^*_{2D} decreases. In addition, increasing the feeding rate causes the increase of the r_{3D} and then r_{2D}, subsequently increasing the actual number of the 2D clusters larger than r^*_{2D}. These operations increase the stable 2D clusters which can become the nuclei of the 2D nuclei growth, resulting in 2D cluster nucleus growth (2DCNG) (as the case of $R=200$ mg/min, Fig. 4(e)).

Finally, we clarify the characteristics of clusters in the plasma flash evaporation process. A typical cluster deposition process developed so far is the ionized cluster beam (ICB) method.[21] The clusters are generated in vacuum by adiabatic expansion process. In this process, ionized clusters are said to break up into individual atoms on the crystal surface after collision and the atoms diffuse on the surface with the migration energy derived from the incident energy resulted from bias voltage. This energy transformation is said to enable low-temperature deposition. For example, Er–Ba–Cu–O thin film deposited at a substrate temperature of 550 °C showed c-axis orientation.[22] However, the clusters often cause damage to film surface because of their high translation energy of larger than 10 eV/cluster.

On the other hand, in the plasma flash evaporation process, thermal energy is supplied to the cluster from thermal plasma, so the cluster is called a ''hot cluster,'' to distinguish it from conventional ''cold'' clusters mentioned above. By quenching from 5000 to 1000 K in a boundary layer, the clusters are kept as thermally activated states without high translation energy such as in the ICB process. These features are expected to enable epitaxial growth with less surface damage. So, hot clusters seem to be preferable in epitaxial growth. Actually, a 1-μm-thick non-spiral growth, monolayer-smooth epitaxial film of YBCO with a full width at half maximum (FWHM) less than 0.14° of the x-ray rocking curve of the (005) peak was successfully deposited at the rate of 16 nm/s.[23] The value of FWHM is one of the smallest values for YBCO films reported so far.[24,25] These facts reconfirm the advantages of hot cluster deposition, especially 2D cluster nucleus growth (2DCNG), overcoming other conventional deposition methods.

Moreover, in our process, it is possible to control the cluster size and feeding rate independently and supply an adequate number of clusters of appropriate size for this epitaxial growth by controlling the feeding rate, distance between plasma torch and substrate, and substrate temperature. Therefore, this process must be named ''hot cluster epitaxy.''

V. CONCLUSIONS

Scanning tunneling microscopy has revealed that spiral growth and two-dimensional cluster nucleus growth occur

under epitaxial film growth conditions in the plasma flash evaporation process. The growth mode is explained by a comparison between the two-dimensional critical radius (r_{2D}^*) derived from the terrace width and the two-dimensional cluster size (r_{2D}) estimated from the three-dimensional cluster size. It is thought that clusters generated in a thermal plasma boundary layer have the activation energy necessary for crystallization and then this process must be called hot cluster epitaxy.

[1] M. K. Wu, J. R. Ashburn, C. J. Torng, P. H. Hor, R. L. Meng, L. Gao, Z. J. Huang, Y. U. Wang, and C. W. Chu, Phys. Rev. Lett. **58**, 908 (1987).
[2] H. Maeda, Y. Tanaka, M. Fukutomi, and T. Asano, Jpn. J. Appl. Phys. Lett. **27**, L209 (1988).
[3] Z. Z. Sheng and A. M. Hermann, Nature (London) **332**, 55 (1988).
[4] Y. Enomoto, T. Murakami, M. Suzuki, and K. Moriwaki, Jpn. J. Appl. Phys. **26**, L1248 (1987).
[5] G. Koren, A. Gupta, E. A. Giess, A Segmuller, and R. B. Laibowit, Appl. Phys. Lett. **54**, 1054 (1989).
[6] T. Terashima, K. Iijima, K. Yamamoto, Y. Bando, and H. Mazaki, Jpn. J. Appl. Phys. **27**, L91 (1988).
[7] H. Busch, A. Fink, and A. Muller, J. Appl. Phys. **70**, 2449 (1991).
[8] K. Terashima, K. Eguchi, T. Yoshida, and K. Akashi, Appl. Phys. Lett. **52**, 1274 (1988).
[9] K. Terashima, H. Komaki, and T. Yoshida, IEEE Trans. Plasma Sci. **18**, 9802 (1990).
[10] Y. Takamura, Y. Hirokawa, H. Komaki, K. Terashima, and T. Yoshida, Physica C **190**, 122 (1991).
[11] K. Terashima, T. Akagi, H. Komaki, and T. Yoshida, J. Appl. Phys. **71**, 3427 (1992).
[12] Y. Takamura, K. Hayasaki, K. Terashima, and T. Yoshida, Plasma Chem. Plasma Process. **16**, 141S (1996).
[13] T. Yoshida, Pure Appl. Chem. **66**, 1223 (1994).
[14] J. Tsujino, H. Yakabe, and Y. Shiohara, Jpn. J. Appl. Phys. **35**, 1706 (1996).
[15] Ch. Gerber, D. Anselmetti, J. G. Bednorz, J. Mannhart, and D. G. Schlom, Nature (London) **350**, 279 (1991).
[16] M. Hawley, I. D. Raistrick, J. G. Beery, and R. J. Houlton, Science **251**, 1587 (1991).
[17] L. Luo, M. E. Hawley, C. J. Maggiore, R. C. Dye, R. E. Muenchausen, L. Chen, B. Schmidt, and A. E. Kaloyeros, Appl. Phys. Lett. **65**, 485 (1993).
[18] W. K. Burton, N. Cabrera, and F. C. Frank, Philos. Trans. R. Soc. London, Ser. A **243**, 299 (1951).
[19] R. F. Cook, T. R. Dinger, and D. R. Clarke, Appl. Phys. Lett. **51**, 454 (1987).
[20] D. G. Schlom, D. Anselmetti, J. G. Bednorz, R. F. Broom, A. Catana, T. Frey, Ch. Gerber, H.-J. Güntherodt, H. P. Lang, and J. Mannhart, Z. Phys. B **86**, 163 (1992).
[21] T. Takagi, I. Yamada, M. Kunori, and S. Kobiyama, *Proc. 2nd Int. Conf. Ion Sources*, Vienna (Österreichische Studiengesellshaft für Atomenergie, Vienna, 1972), p. 790.
[22] Y. Kawagoe, K. Yamanishi, M. Tanaka, K. Imada, and K. Sato, Nucl. Instrum. Methods Phys. Res. B **59/60**, 1426 (1991).
[23] Y. Takamura, N. Yamaguchi, K. Hayasaki, T. Hattori, K. Terashima, and T. Yoshida (unpublished).
[24] S. William, J. Q. Zheng, M. C. Shih, X. K. Wang, S. J. Lee, E. D. Ripert, S. Maglic, H. Kajiyama, D. Segel, P. Dutta, R. P. H. Chang, and J. B. Ketterson, J. Appl. Phys. **72**, 4798 (1992).
[25] J.-H. Xu, G.-G. Zheng, A. M. Grishin, B. M. Moon, K. V. Rao, and J. Moreland, Appl. Phys. Lett. **64**, 1874 (1992).